

Lattice dynamics of pressure-polymerized phases of C₆₀: A neutron scattering investigation

S. Rols, J. Cambedouzou, J.-L. Bantignies, F. Rachdi, and J.-L. Sauvajol

Groupe de Dynamique des Phases Condensées (UMR CNRS 5581), Université Montpellier II, 34095 Montpellier Cedex 5, France

V. Agafonov

Laboratoire de Chimie Physique (E.A. PIMIR 2098), Faculté de Pharmacie de l'Université de Tours, 37200 Tours, France

A. V. Rakhmanina and V. A. Davydov

Institute of High Pressure of the RAS, 142 092 Troitsk, Moscow Region, Russian Federation

B. Hennion and R. Kahn

Laboratoire Léon Brillouin, C.E.-Saclay, 91191 Gif sur Yvette Cedex, France

(Received 15 October 2003; revised manuscript received 11 June 2004; published 8 September 2004)

We report on inelastic neutron scattering (INS) investigations of the dimer (*D*) state and of the orthorhombic (*O*), tetragonal (*T*), and rhombohedral (*R*) polymeric phases of C₆₀ obtained upon high pressure-high temperature treatments. The neutron data confirm that the low-frequency profile of the inelastic neutron scattering spectra is highly sensitive to the structure of the phase. The differences between the spectra are discussed in terms of structure-specific low-energy modes which are driven by the degree of polymerization.

DOI: 10.1103/PhysRevB.70.104302

PACS number(s): 63.20.-e, 63.22.+m

I. INTRODUCTION

The C₆₀ fullerite crystallizes into the face-centered cubic (fcc) phase at ambient conditions. This phase is known to be a plastic phase in which the C₆₀ molecules rotate freely around their center of mass. On cooling below 260 K, this rotation freezes and the system transforms to the simple cubic phase.^{1,2} However, C₆₀ is known to form polymeric compounds under certain conditions. Of particular interest are the crystalline polymerized phases that can be obtained by high-pressure high-temperature treatment (HPHTT) of fullerite C₆₀. Under this treatment, the neutral C₆₀ molecules polymerize by forming between one and six [2+2] cycloaddition interball connections in which parallel (6,6) bonds on adjacent C₆₀'s are connected by a pair of carbon-carbon (C-C) bonds. The polymerized structures obtained by this route include dimers (*D*), orthorhombic (*O*) one-dimensional (1D) chains, tetragonal (*T*), and rhombohedral (*R*) two-dimensional (2D) lattices³⁻⁵ (Fig. 1). The determination of the vibrational features of these phases remains an experimental challenge, the main problem being the difficulty of obtaining samples with well-defined molecular fractional composition and high purity. Up to now, the simultaneous presence of the different polyfullerenes in the sample has made the task of spectra interpretation very complicated. These samples, as a rule, represented the mixture of different polymerized phases—or solid solutions of polyfullerenes—with indefinite fractional composition.⁵⁻⁸ Recently, successful synthesis of practically pure samples of the *O*, *T* and *R* phases allowed investigation of their structural (x-ray diffraction) and vibrational (infrared and Raman spectroscopy) properties.^{10,9} In Fig. 2 of Ref.10 are shown the x-ray diffraction (XRD) patterns of the *O*, *T*, *R* phases and of the *D* states. The comparison with calculated XRD patterns shows that there is practically no unindexed diffraction peak in the experimental diagrams, proving that the samples are almost

single phased. The conditions for pure dimeric state synthesis are, however, not yet precisely known. Nevertheless the x-ray diffraction (XRD) pattern of the *D*-state is different enough from those of the other phases to be used as a tool to identify this particular state. The vibrational spectrum of solid C₆₀ ranges from 0 to 200 meV. It is well known that it can be divided into two clearly separated zones, i.e., the intramolecular vibration range (30–200 meV), and the intermolecular vibration range (0–8 meV), showing a gap region between 8 and 30 meV². The effect of polymerization and dimerization involves modifications of the spectra in the complete range.

The intramolecular frequency range (e.g., 30–250 meV) of the infrared (IR) and Raman spectra of the *O*, *T*, *R* and *D* HPHTT phases has been studied experimentally at room temperature¹⁰ and the spectra were discussed, based on group-theoretical analysis of pristine C₆₀ and its molecular clusters. Recently, very accurate studies of the IR active vibrational modes of the polyfullerenes were carried out using quantum molecular dynamics simulations.¹¹⁻¹⁴ The assignment of the vibrational spectra of the different phases allows one to consider the IR and Raman spectra of the crystalline polymerized phases as characteristic of these phases.

The polymerization of C₆₀ leads to drastic changes in the low frequency dynamics (0–30 meV) where typical interball modes (ball stretching, torsions etc.) and molecular lattice modes (acoustic phonons, librations) show up. The study of the low-frequency excitations of pressure-induced polymerized phases of C₆₀ has been performed using far-infrared spectroscopy,¹²⁻¹⁴ Raman spectroscopy,^{10,15} and inelastic neutron scattering experiments.^{15,16} In investigations by high-resolution far-infrared transmission, no low-energy mode was observed in the 2–10 meV range.¹²⁻¹⁴ However, a Raman study of pure pressure-polymerized samples¹⁰ was carried out in the 6–225 meV range, and the Raman spectrum of the dimer was found to be characterized by a peak at

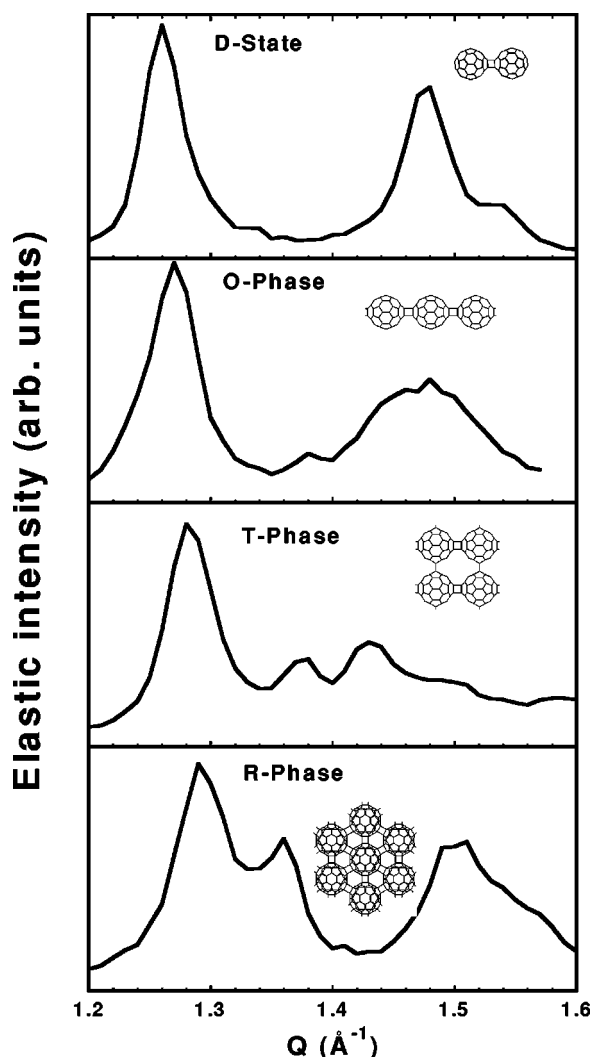


FIG. 1. The elastic $S(Q, \omega=0)$ part of the neutron scattering spectra, and a schematic representation of the corresponding structure. From top to bottom: dimer, O polymer, T polymer, and R polymer of C_{60} .

11.7 meV. This feature was assigned to the total symmetric interball vibration of $[C_{60}]_2$. By neutron investigations, it was found that 1D polymerization of charged C_{60} in the RbC_{60} phase leads to the appearance of new features in the 0–8 meV range as well as in the 8–30 meV gap related to interchain and interball vibrations.¹⁷ The INS spectrum of the 1D-polymer phase of RbC_{60} and the INS spectrum of a polymeric phase of C_{60} obtained at 1.2 GPa and 600 K exhibited a similar profile. According to their calculations, the authors assigned this particular HPHTT phase as mainly containing linear chains of cages polymerized via the [2+2] cycloaddition reaction.¹⁵ Another INS study of a HPHTT C_{60} polymer obtained at 2.1 GPa and 620 K showed the presence of two strong peaks at 12.8 and 16.6 meV, with a weak component at 5.2 meV.¹⁶ These peaks were tentatively assigned to interball vibrations of the infinite chains of C_{60} , but the absence of data about the exact structure of this sample did not permit further conclusions to be drawn.¹⁶ The unavailability of pure polymeric samples is the main reason for the absence of a

systematic INS study of the HPHTT phases up to now. This paper presents an investigation of a complete systematic study of the vibrational characteristics of the polymers (O , T and R) phase and dimer (D) state of C_{60} obtained by HPHTT with a high degree of purity and almost monophased. We focus our study on the low-energy range of the vibrational spectra which mainly comprises the interball vibrations, using an inelastic neutron scattering technique.

II. SAMPLES AND EXPERIMENTAL SETUP

A. Samples

All polymeric phases were produced by high-pressure high-temperature treatment (HPHTT) of fullerite C_{60} in piston-cylinder and toroid-type high pressure devices. High-pure (99.98%) twice-sublimed small-crystalline fullerite C_{60} supplied by Term USA was taken as a starting material. The initial powder was stored inside vacuum-sealed ampoules and was opened just before use. This procedure almost entirely prevents the intercalation of oxygen in the bulk of material which could react with C_{60} at high temperature. The P , T parameters and times of HPHTT chosen for synthesis of high-pressure phases have been published elsewhere.¹⁰ Raman and x-ray diffraction characterizations of all samples confirm the purity and the homogeneity of the polymeric phases obtained this way. It should be noted that we did not find the conditions for pure dimeric phase synthesis. Consequently, the dimeric state studied in this work is a sample with a $[C_{60}]_2$ content of about 80 mole %. A mass of about 300 mg (200 mg) of each pressure-polymerized (dimerized) phase was prepared in powder form for the inelastic neutron scattering (INS) investigations.

B. The inelastic neutron scattering experiments

Inelastic neutron scattering (INS) experiments were performed on powdered samples using two complementary techniques. A first set of experiments was carried out at 200 K on the triple-axis spectrometer (4F2) installed on the cold source of the Orphée reactor at the Laboratoire Léon Brillouin.¹⁸ The use of a triple-axis spectrometer allows one to collect data either at constant Q momentum transfer (energy scans) or at constant energy transfer $\hbar\omega$ (Q scans). This experimental setup provides an efficient way to determine the scattering function $S(Q, \omega)$ in the (Q, ω) space. Q scans were performed at elastic scattering ($\hbar\omega=0$) in order to derive the elastic structure factor for comparison with diffraction diagrams (see Fig. 1). The energy scans were performed with a constant final wave vector $k_f=1.97 \text{ \AA}^{-1}$ giving an energy resolution of about 0.4 meV at constant $Q=3.5 \text{ \AA}^{-1}$ transfer. Another set of INS experiments were performed at room temperature on the cold time-of-flight (TOF) spectrometer (MiBeMol) at incident wavelength 5 \AA in a scattering angle ranging from 12° to 147° . This setup allows one to explore a Q range from 0.26 – 2.41 \AA^{-1} at elastic scattering (0.45 – 2.74 \AA^{-1} at 2 meV). After classical treatments,¹⁹ one obtains the generalized density of states (GDOS). For coherent scattering such as carbon, this is achieved within the framework of the incoherent approximation.^{20,21} The validity

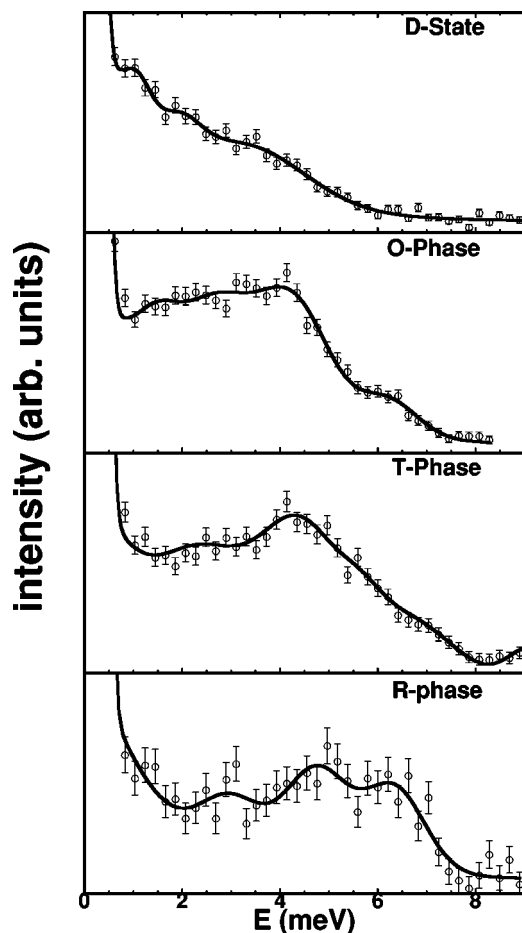


FIG. 2. The inelastic $S(Q, \omega)$ part of the neutron scattering spectra. From top to bottom: dimer, O polymer, T polymer, and R polymer of C_{60} .

of the incoherent approximation depends on the ratio between the volume in the Q space probed during the experiment to the volume of the first Brillouin zone of the compound studied. The larger this ratio, and the better the approximation. For a lattice with a typical 10 \AA lattice parameter, the volume of the first Brillouin zone gives a value of the order of $(2\pi/10)^3 = 0.25 \text{ \AA}^{-3}$. For an excitation at 2 meV , the volume in Q space probed is of the order of 86 \AA^{-3} giving a ratio of about 346. Such a value indicates that the incoherent approximation is meaningful. The $S(Q, \omega)$ spectra (see Fig. 2) have been fitted with a set of Gaussian components added to a delta function and a lorentzian contribution. The latter function was included to account for a quasielastic component observed at low frequency in each spectrum. The origin of this quasielastic signal is not clear, but the fact that it is present in the spectra whatever the sample and its structure leads to the conclusion that it is related to an experimental artefact. Such a quasielastic component is not observed in the high-resolution TOF spectra as indicated by the weak intensity of the GDOS at very low frequency (see Fig. 3). However, it is necessary to take into account such a component in order to obtain a good fit of the $S(Q, \omega)$ profile. The fits of the spectra were obtained by adding the smallest number of Gaussian components. In this sense, the solid lines in

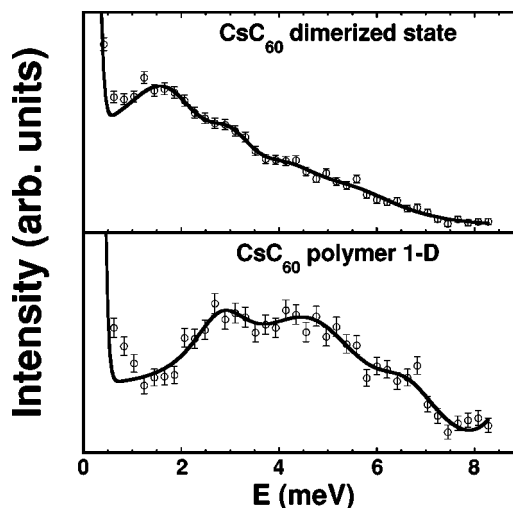


FIG. 3. The inelastic $S(Q, \omega)$ part of the neutron scattering spectra of dimer CsC_{60} (top) and 1D polymer phase of CsC_{60} (bottom).

Fig. 2 can be viewed as guides to the eyes and the different components will not be shown. For an easy comparison of the two data sets, we derived the GDOS from the $S(Q, \omega)$ measured on the triple-axis spectrometer. For that, the elastic and quasielastic contributions were removed from the experimental spectra, and the GDOS was obtained using the usual expression:

$$G(\omega) \sim \frac{\omega S(Q, \omega)}{Q^2 [n(\omega, T) + 1]}, \quad (1)$$

where $n(\omega, T)$ is the Bose factor at temperature T . Deriving the GDOS for a pure coherent scatterer and using a single Q value might be taken with high care. One has to keep in mind that this will not give an absolute estimation of the density of states, but this function is derived to provide a useful quantity that can be compared with the GDOS derived from TOF experiments and from calculations.

III. EXPERIMENTAL RESULTS

Figure 1 displays the elastic part $S(Q, \omega=0)$ of the neutron scattering spectra measured in the $1.2\text{--}1.6 \text{ \AA}^{-1}$ Q range at 200 K for the dimer state and polymer phases of C_{60} . These diagrams were recorded to test the homogeneity and the purity of the large mass of samples used for the INS experiments. Despite the poor Q resolution, the overall profile of the diagrams are sufficiently distinct from each other in this Q range to distinguish the different phases and allow a correct characterization of the samples. The correspondence between these diagrams and those obtained on smaller amounts of sample by x-ray diffraction¹⁰ ensures that the large mass of each sample used in the neutron experiment relates to an homogeneous specific pressure-polymerized phase of C_{60} . Therefore, the crystal structures of our samples were assumed to be the same as those determined from previous structural studies,^{22–24} which give a rhombohedral structure for our R phase with space group $R3m$, composed of three trigonal 2D layers ($P3m1$ symmetry) stacked rhom-

bohedrally in the sequence *ABC* with C_{60} molecules keeping the same orientation along the *c* axis and held together by van der Waals forces. The crystal structure of the *T* phase depends on the conditions of synthesis and can have either *Immm* orthorhombic (pseudotetragonal)²³ or $P4_2/mmc$ true tetragonal structure.²⁴ Our method leads, rather, to the $P4_2/mmc$ structure of the *T* phase. The exact crystal structure of the *O* and dimer phases are not known. However, the study performed on the multidomain crystal of the *O* phase led to an orthorhombic lattice with *Pmnn* symmetry and containing C_{60} chains.²⁵ Finally, the dimer phase crystallizes into the cubic $Fm\bar{3}m$ symmetry, which supposes that the dimers are packed in a disordered manner.²⁶ The raw experimental data $S(Q, \omega)$ measured at 200 K on the triple-axis spectrometer are reported in Fig. 2. All these responses have been measured at $Q=3.5 \text{ \AA}^{-1}$. As expected, the low-frequency profile of the dynamic structure factor $S(Q, \omega)$ is found to be sample-dependent. In particular, a general energy upshift of the $S(Q, \omega)$ intensity is observed when increasing the degree of polymerization (e.g., from the *D* state to the *R* phase). The $S(Q, \omega)$ of the *D* state and *O* phase are found to be very similar to the $S(Q, \omega)$ obtained for the dimer-state and *O* phase of CsC_{60} Ref. 27 (Fig. 3). These early results were obtained at 200 K on the same spectrometer within the same conditions as those used in the present experiments, and their INS profile was fitted using the same number of components. The similarity between the two *D* states and the two *O*-phase profiles shows that the structure of the phonon bands are equivalent and characteristic of the structure of the polyfullerene phase studied. The position of the components are, however, found to be located at a higher frequency for the CsC_{60} phases than for their pressure-polymerized homologues. The peaks are located close to ~ 1.5 , 2.7 , and 4.1 meV in the CsC_{60} dimer state²⁷ against ~ 1 , 2 , and 3.4 meV in the pressure-dimerized state. The low-frequency peaks are located at ~ 2.9 and ~ 4.6 meV in the CsC_{60} *O* phase²⁷ against ~ 2.3 and ~ 4.2 meV in the pressure-polymerized *O* phase.

It is well known that the C_{60} molecules are connected by a single carbon-carbon bond²⁸ for the dimer state of CsC_{60} , by contrast to the pressure-dimerized state where a cyclobutanelike double bridge links the two C_{60} balls. One would have expected that a lower number of bond per dimer in CsC_{60} would have led the interball modes of the charged dimers to occur at lower frequency than their equivalent for the neutral dimers and change the phonon bands structure significantly, in contrast to what we observe. On the other hand, the interaction between the singly charged C_{60} molecules and the Cs cations should lead to a hardening of the force constants. In consequence, the experimental upshift observed between the $S(Q, \omega)$ of the CsC_{60} *D* state with respect to that of the pressure *D* state can be explained by this latter effect that overcompensates the changes due to the difference in number of bonds. This is confirmed by the observation of such upshift in the CsC_{60} *O* phase with respect to the pressure *O* phase while the number of bonds is the same in both compounds.

The generalized density-of-states of the pressure-polymerized samples is displayed in Fig. 4. A good agree-

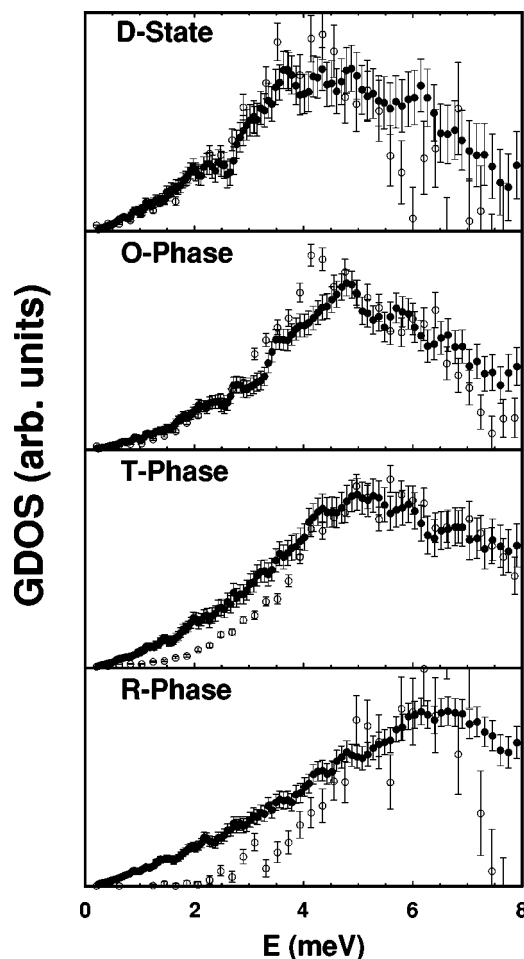


FIG. 4. The triple axis (\circ) and TOF (\bullet) derived GDOS. From top to bottom: dimer, *O* polymer, *T* polymer, and *R* polymer of C_{60} .

ment is found between both instrument-derived GDOS, especially for the dimer state and for the polymeric *O* phase: the positions of the principal features are located around the same positions and a general upshift of the spectral weight is observed when increasing the degree of polymerization. This agreement ensures the validity of our approach despite the weak signal-to-noise ratio due to the weak neutron scattering cross section of carbon atoms, and the relatively weak mass of the samples used in the experiments (~ 200 mg). TOF results give a more precise profile of the GDOS at very low energy than triple-axis experiment results, especially because the signal is not disturbed by the presence of the spurious quasielastic component. Let us focus our discussion on the profile of the TOF-derived GDOS for all the samples, this spectrum being referred to in the following as GDOS or density of states.

In the pressure-dimerized state, the density of states is dominated by a broad doublelike component centered around 4.5 meV, with a small shoulder located around 2.3 meV. This spectrum strongly resembles that obtained on a RbC_{60} phase by Schober and collaborators.²⁹ These authors used a hybrid force-constant approach to calculate the GDOS, and the phonon dispersion relations, of the RbC_{60} dimer state, by considering a $[2+2]$ bonded dimer (model D1 in Ref. 29).

This model predicts three librational bands at approximately 3, 4, and 5 meV.²⁹ By assuming a systematic downshift of these bands in pressure-dimer state with respect to AC_{60} dimer state, one could assign the strong and broad feature around 4.2 meV and the small bump at 2.3 meV as due mainly to contributions from librations characteristic of a molecular system bound by van der Waals interactions [the C_{60} libron is measured at ~ 2 meV in the ordered low-temperature phase of C_{60} (Ref. 30)]. In addition, the calculated dispersion curves (Fig. 7 in Ref. 29) predict contributions of acoustic modes (at the edge of the Brillouin zone) in the same energy range. A few years ago, Porezag and co-workers¹¹ calculated the low-energy modes for an isolated $[2+2]$ dimer using density-functional based methods. Odd-parity libration modes were predicted at 2.7 and 4.2 meV, and the torsion mode — where the balls are twisted around the dimer axis — is predicted at 2.8 meV. All these bands are weakly dispersive so that they certainly contribute to the 4.5 meV dominant broad band and to the 2.3 meV shoulder of the DOS of the pressure-dimerized state. However, a careful observation of the low-frequency part of the D -state $S(Q, \omega)$ spectrum (see Fig. 2) reveals an additional intensity around 1 meV that is not predicted in the Porezag calculations. By comparison with the CsC_{60} dimer state, we tentatively attribute this component to libration of the dimer molecule as a whole. In this sense, this mode is a lattice mode. Consequently it is more sensitive to the lattice disorder than intramolecular librations. The pressure-dimer phase being an orientational disordered phase,^{10,26} this later librational mode should be very sensitive to the rotational disorder of the dimeric units, so that it must be anharmonic. Such orientational disorder can be in part responsible for the absence of a clear signature from these modes in the TOF-derived GDOS, the experiment being performed at relatively high temperature (300 K). To address this question, the study of the temperature dependence of INS spectrum is scheduled. However, one cannot also exclude that the maximum of the dynamical structure factor of this mode arises in a Q value outside the Q range of TOF experiments ($Q < 2.6 \text{ \AA}^{-1}$ for $\omega = 1$ meV), leading to the absence of this contribution [by contrast $S(Q, \omega)$ in which this mode appears is measured at $Q = 3.5 \text{ \AA}^{-1}$].

As expected, the profiles of the GDOS (Fig. 4) for the pressure-polymerized orthorhombic phase are significantly different from those measured in the pressure-dimerized

state. First, the dominant feature of the GDOS is located at ~ 4.75 meV, and the low-frequency shoulder is no longer observed. The dominant signal is close to the one obtained for the RbC_{60} O phase²⁹ where the main peak, located just below 5 meV, is assigned to C_{60} librations around the chain axis. The absence of relevant features at low frequency might reflect a hardening of the acoustic modes compared to the dimer state, with librionic branches having stronger dispersion character along the chain direction.

The hardening of the main feature of the GDOS is even more pronounced for the T and R phases, the most significant shift occurring for the rhombohedral pressure-polymerized phase where the main component is observed around 6 meV. In line with the previous discussion that explained the differences between the D state and the O phase, one could think of a general hardening of the acoustic and librionic modes as a function of the number of $[2+2]$ bonds per molecule: one in the dimer state, two for the 1D polymer phase, four in the 2D tetragonal phase, and six in the 2D rhombohedral phase. Actually, the hardening of the lattice from the T to the R phase may have the consequence of upshifting the main peak of the GDOS from ~ 5.5 to ~ 6.5 meV. Such a peak seems appropriate to identify the degree of polymerization of the sample under study. Further calculations are, however, needed in order to assign these contributions correctly.

IV. CONCLUSION

We have obtained the low-frequency density-of-states of pressure-dimerized state and orthorhombic, tetragonal, and rhombohedral pressure-polymerized phases of C_{60} . These profiles show significant differences which are discussed in terms of hardening of the interball translational and librionic modes as a function of the degree of polymerization. In particular, a peak in the density of states located around 6.5 meV is found to be characteristic of the R phase. In order to assign properly these different low-frequency excitations, inelastic neutron measurements in a wide temperature range (10–600 K), and calculations of the dynamics of the C_{60} molecules in these different lattices are in progress.

ACKNOWLEDGMENTS

This work was supported by the NATO Science Program (Grant No. PST. CLG. 979714) and the Russian Foundation for Basic Researches (Grant No. 03-03-32640).

¹P. A. Heiney, J. E. Fischer, A. R. McGhie, W. J. Romanow, A. M. Denenstien, J. P. McCauley, Jr., A. B. Smith III, Phys. Rev. Lett. **66**, 2911 (1991).

²M. S. Dresselhaus, G. Dresselhaus, and P. C. Eklund, *Science of Fullerenes and Carbon Nanotubes* (Academic Press, New York, 1996).

³A. M. Rao, P. Zhou, K. A. Wang, G. T. Hager, J. M. Holden, Y. Wang, W. T. Lee, X.-X. Be, P. C. Eklund, D. S. Cornett, M. A. Duncan, and I. J. Amster, Science **259**, 955 (1993).

⁴M. Nuñez-Regueiro, L. Marques, J.-L. Hodeau, O. Berthoux, and M. Perroux, Phys. Rev. Lett. **74**, 278 (1995).

⁵Y. Ywasa, T. Arima, R. M. Fleming, T. Siegrist, O. Zhou, R. C. Haddon, L. J. Rothberg, K. B. Lyons, H. L. Carter, Jr., A. F. Hebard, R. Tycko, G. Dabbagh, J. J. Krajveski, G. A. Thomas, and T. Yagi, Science **264**, 1570 (1994).

⁶C. S. Sundar, P. Ch. Sahu, V. S. Sastry, G. V. Rao, V. Sridharan, M. Premila, A. Bharathi, Y. Hariharan, and T. S. Radhakrishnan, Phys. Rev. B **53**, 8180 (1996).

- ⁷A. M. Rao, P. C. Eklund, J.-L. Hodeau, L. Marques, and M. Nuñez-Regueiro, *Phys. Rev. B* **55**, 4766 (1997).
- ⁸A. M. Rao, P. Zhou, K. A. Wang, G. T. Hager, J. M. Holden, Y. Wang, W. T. Lee, X.-X. Be, P. C. Eklund, D. S. Cornett, M. A. Duncan, and I. J. Amster, *Appl. Phys. A: Mater. Sci. Process.* **64**, 231 (1997).
- ⁹K. Kamarás, Y. Ywasa, and L. Forró, *Phys. Rev. B* **55**, 10 999 (1997).
- ¹⁰V. A. Davydov, L. S. Kashevarova, A. V. Rakhmanina, V. M. Senyavin, R. Céolin, H. Szwarc, H. Allouchi, and V. Agafonov, *Phys. Rev. B* **61**, 11 936 (2000).
- ¹¹D. Porezag, M. R. Pederson, Th. Frauenheim, and Th. Kohler, *Phys. Rev. B* **52**, 14 963 (1995).
- ¹²V. C. Long, J. L. Musfeldt, K. Kamarás, G. B. Adams, J. B. Page, Y. Iwasa, and W. E. Mayo, *Phys. Rev. B* **61**, 13 191 (2000).
- ¹³Z. T. Zhu, J. L. Musfeldt, K. Kamarás, G. B. Adams, J. B. Page, V. Davydov, L. S. Kashevarova, and A. V. Rakhmanina, *Phys. Rev. B* **65**, 085413 (2002).
- ¹⁴Z. T. Zhu, J. L. Musfeldt, K. Kamarás, G. B. Adams, J. B. Page, L. S. Kashevarova, A. V. Rakhmanina, and V. Davydov, *Phys. Rev. B* **67**, 045409 (2003).
- ¹⁵B. Renker, H. Schober, R. Heid, and P. V. Stein, *Solid State Commun.* **104**, 527 (1997).
- ¹⁶A. I. Kolesnikov, I. O. Bashkin, A. P. Moravsky, M. A. Adams, M. Prager, and E. G. Ponyatovsky, *J. Phys.: Condens. Matter* **8**, 10 939 (1996).
- ¹⁷B. Renker, H. Schober, F. Gompf, R. Heid, and E. Ressouche, *Phys. Rev. B* **53**, R14 701 (1996).
- ¹⁸Laboratoire Léon Brillouin, CEA-Saclay, 91191 Gif-sur-Yvette Cedex, FRANCE, www-llb.cea.fr
- ¹⁹M. Bée, *Quasi-elastic Neutron Scattering: Principles and Applications in Solid State Chemistry, Biology and Material Science* (Adam Hilger, Bristol, 1988).
- ²⁰V. S. Oskotskii, *Sov. Phys. Solid State* **9**, 420 (1967).
- ²¹M. M. Bredov, *Sov. Phys. Solid State* **9**, 214 (1967).
- ²²X. Chen, S. Yamanaka, K. Sako, Y. Inoue, and M. Yasukawa, *Chem. Phys. Lett.* **356**, 291 (2002).
- ²³X. Chen and S. Yamanaka, *Chem. Phys. Lett.* **360**, 501 (2002).
- ²⁴B. Narymbetov, V. Agafanov, V. A. Davydov, L. S. Kashevarova, A. V. Rakhmanina, A. D. Dzyabchenko, V. I. Kovalov, and R. Ceolin, *Chem. Phys. Lett.* **367**, 157 (2003).
- ²⁵R. Moret, P. Launois, P.-A. Persson, B. Sundqvist, *Europhys. Lett.* **66**, 55 (1997).
- ²⁶R. Moret, P. Launois, T. Wagberg, B. Sundqvist, V. Agafonov, V. A. Davydov, and A. V. Rakhmanina, *Eur. Phys. J. B* **37**, 25 (2004).
- ²⁷J.-L. Sauvajol, E. Anglaret, R. Aznar, D. Bormann, and B. Hennion, *Solid State Commun.* **104**, 387 (1997).
- ²⁸G. Oszlányi, G. Bortel, G. Faigel, L. Granasy, G. M. Bendele, P. W. Stephens, and L. Forró, *Phys. Rev. B* **54**, 11 849 (1996).
- ²⁹H. Schober, A. Tolle, B. Renker, R. Heid, and F. Gompf, *Phys. Rev. B* **56**, 5937 (1997).
- ³⁰J. R.D. Copley, D. A. Neumann, R. L. Cappelletti, and W. A. Kamitakahara, *J. Phys. Chem. Solids* **53**, 1353 (1992).